IEEE Access
Multidisciplinary | Rapid Review | Open Access Journal

Received 12 August 2023, accepted 5 September 2023, date of publication 11 September 2023,
date of current version 18 September 2023.

Digital Object Identifier 10.1109/ACCESS.2023.3314379

RESEARCH ARTICLE

Adaptive Dosing Control System Through ARIMA Model for Peristaltic Pumps

DAVIDE PRIVITERA[1,2], STEFANO BELLISSIMA[2], AND SANDRO BARTOLINI[1]
[1]Department of Information Engineering and Mathematics, University of Siena, 53100 Siena, Italy
[2]Pharma Integration, 53100 Siena, Italy

Corresponding author: Davide Privitera (privitera@diism.unisi.it)

ABSTRACT Peristaltic pumps play a crucial role in the pharmaceutical industry, offering advantages such as reduced cross-contamination risks and ease of use. However, their dosing precision often lags behind other devices like volumetric pumps. This study investigates the underlying causes of this phenomenon and proposes effective mitigation strategies to enhance accuracy. Notably, two novel aspects are explored: the underlying causes of dosing variation and compensation systems on precision filling. Through comprehensive analysis, the impact of product temperature on accuracy is unveiled, resulting mainly from variations that alter the elastic properties of the pipe material and lead to significant deviations in dosed volume. Therefore, temperature stabilization becomes imperative for optimal performance. Additionally, the Adaptive Dosing Control System (ADCS) based on time series prediction is introduced, enabling real-time compensation of volume delivery. The filling system is considered as a black box, allowing potential application of these findings on other similar industrial setups. Extensive experiments on state-of-the-art robotic production lines validate the ADCS's stability and effectiveness, demonstrating up to a 30% improvement in accuracy. In conclusion, this research sheds light on the critical relationship between product temperature and peristaltic pump dosing, while the ADCS represents an advancement in precision filling technology. These results hold potential for enhancing precision, reducing wastage, and improving product quality in the pharmaceutical industry and other precision filling applications.

INDEX TERMS Peristaltic pumps, adaptive control system, forecasting compensatory control, ARIMA.

I. INTRODUCTION AND MOTIVATION

Filling devices are widely used in industries as they allow for the handling of fluids, both for conveying and dispensing purposes. Traditional filling technologies employed in fields such as pharmaceuticals, chemicals, and food and beverage industries include piston pumps and time-pressure systems. While piston pumps are popular for their precision, they have certain drawbacks in specific applications [1].

A piston pump consists of various mechanical components, such as valves and seals, which come into direct contact with the product. This poses a problem in certain scenarios as these components need to be disassembled, cleaned, and reassembled between uses to prevent cross-contamination. Moreover, the mechanical structure of piston pumps makes them fragile and prone to damage. Additionally, these pumps can impose stress on bio-pharmaceutical products [2].

In recent decades, peristaltic filling technology has gained prominence due to new challenges and stricter validation requirements, especially in the pharmaceutical industry [1]. In peristaltic pumps, the product only comes into direct contact with a single piece of tubing, which can be easily cleaned or replaced after use. This tube, typically made of elastomers or thermoplastics, is housed in a circular seat on the pump body and is compressed by the rotational action of two or more rollers, as shown in Figure 1. After passing the first roller, the tube regains its original shape, creating a vacuum and subsequent suction. The aspirated fluid enters the cavity formed between the rollers and, during rotation, is pushed towards the outlet by the compression of the next roller.

The associate editor coordinating the review of this manuscript and approving it for publication was Qi Zhou.

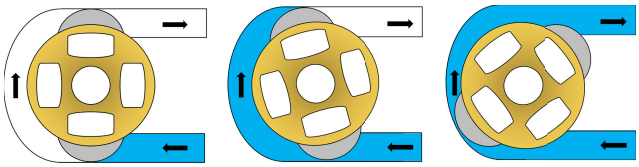

FIGURE 1. Peristaltic pump working principle.

The ability to easily change the tube in contact with the product makes peristaltic pumps an attractive alternative for dispensing bio-pharmaceutical injectable drugs, significantly reducing the risk of cross-contamination. Furthermore, by adjusting the tube size, a wide range of filling volumes (ranging from 0.1 to 250 ml) can be easily managed. The setup and calibration procedure can be completed in under five minutes, and the introduction of new silicone materials for the tubes has improved their handling of aggressive products [3].

As stated in [3] and [4], one major concern with peristaltic pumps is their fill accuracy, which is particularly challenging at low fill volumes. Achieving high accuracy is crucial in the pharmaceutical industry due to quality compliance requirements and the cost of the drug fluid. Improving these capabilities can bring several benefits, not only by promoting the use of peristaltic pumps but also by optimizing costs through potential product waste reduction.

Therefore, the purpose of this investigation is to study the factors that contribute to the accuracy of peristaltic pumps with the aim of improving it through the application of an adaptive runtime filling compensation strategy based on time series prediction. This approach enables real-time compensation of the volume delivered by the filling system by leveraging predictions based on previously observed volumes.

Similar techniques have been presented in the past [5] and are known as Forecasting Compensatory Control (FCC) systems. The main idea behind these systems is to compensate for errors through software rather than investing significant resources in mechanical improvements, which often yield limited results. Notably, this method can not only compensate for repetitive, systematic errors but also predict non-repetitive stochastic variations, enabling the correction of correlated dynamic inaccuracies. In their work [5], Wu and Ni presented examples of compensation applications, such as improving workpiece straightness in end milling. In this case, a laser sensor was used to evaluate the flatness of a machined object, and any errors were compensated by adjusting the position of the milling tool during the process.

Similar results are presented in [6], [7], [8], and [9], where error compensation methods for milling machine tools are explored. The authors emphasize the fundamental importance of developing a precise error model, which is often a complex task but necessary for achieving performance improvements.

In addition to milling machines, other manufacturing processes have been proposed, such as integrated circuit production [10], precision multi-axis motion control systems with contour performance orientation [11], and additive manufacturing for thermal distortion compensation [12]. Furthermore, recent research has explored the application of different control techniques in various domains, including complex systems [13] and adaptive control [14], [15].

All these works demonstrate that a careful and targeted study of specific processes enables the development of compensation systems that optimize accuracy performance. However, a lack of research exists in the literature concerning compensation studies specifically focused on industrial filling systems, which exhibit distinctive characteristics compared to other manufacturing processes. Although our investigation primarily concentrates on precision filling systems for pharmaceutical applications, the practical benefits of such an approach can extend to diverse domains such as food and beverages, as well as cosmetics. Therefore, a thorough investigation is necessary to understand the mechanisms influencing accuracy and to determine whether compensation systems can effectively enhance performance.

In this context, both AI and statistical methods have been considered. AI techniques have gained widespread adoption across various fields due to their effectiveness and versatility. AI methods, such as artificial neural networks (ANNs), support vector machines (SVMs), and deep learning algorithms, have shown remarkable success in predictive modeling tasks. For example, in [16] and [17] the authors discuss the application of Radial Basis Function Neural Networks (RBF NN) for system prediction, while [12] explores the use of AI for predicting thermal distortion. These studies demonstrate the potential of AI techniques in optimizing different systems. Although AI techniques offer promising avenues for investigation, for the current study, the Autoregressive Integrated Moving Average (ARIMA) [18] model for time series prediction was initially chosen due to several advantages it offers. Firstly, ARIMA is a well-established method with a proven track record of success in time series prediction. It has been extensively used in various fields such as finance, economics, and engineering, consistently providing accurate predictions in numerous scenarios. Its performance is well-documented, and it is widely recognized as a reliable method for time series forecasting. Secondly, ARIMA is a straightforward and explainable system. The algorithm is based on linear equations and a set of assumptions that are easy to understand and interpret. This aspect is particularly important in industrial scenarios where stakeholders need to comprehend the underlying mechanisms of the prediction models applied in complex cyber-physical systems. Lastly, ARIMA has been also shown to outperform other strategies in various domains [19], [20].

All the experiments reported in this paper have been conducted at Pharma Integration [21], a company focused on the development of highly precise and efficient filling lines using robotic technology, in compliance with the recently published Annex 1 of the Good Manufacturing Practices guidelines [22]. The company's mission aligns perfectly with the current fourth industrial revolution, which

is characterized by the integration of advanced technologies into the manufacturing process.

Ultimately, this work presents the following major contributions:

- A significant relationship between product temperature and dosing accuracy is unveiled through a comprehensive analysis. The effects of product density, thermal expansion, and the elastic properties of the tube material are considered, leading to the novel discovery that variations in product temperature directly impact the dosed volume. Contrary to common assumptions, this research highlights the pivotal role of changes in tube elasticity in influencing dosed volumes, providing valuable implications for optimizing dosing accuracy in various industrial dosing setups.
- To address challenges arising from inherent noise in the dosing system, an adaptive run-time filling compensation strategy based on time series prediction is introduced. This approach, referred to as the Adaptive Dosing Control System (ADCS), enables real-time compensation of the filling system's volume delivery. By treating the system as a black box, this approach offers the advantage of potential applicability to diverse dosing setups beyond the specific one studied, making it highly suitable for various industrial applications.
- A comprehensive analysis of predictive model parameters specific to the filling system context is conducted. By exploring various model configurations and conducting thorough parameter analysis, it is found that an auto-regressive (AR) model effectively captures the underlying patterns and dynamics of the dosing system. The AR model's ability to adapt to changing dynamics and capture sequential dependencies has proven highly effective in improving dosing accuracy.
- The insights and innovations presented offer specific practical implications for the pharmaceutical industry and other applications relying on precision filling technology. Optimizing dosing accuracy and compensating for temperature effects open possibilities for enhanced efficiency, reduced wastage, and improved product quality in real production environments.

II. CONTEXT OF THE ADCS

This section provides details about the main elements involved in the setting of the ADCS. Specifically, the architecture of an industrial dosing system, the adopted hardware/software setup, and the investigation methodology are illustrated.

A. SYSTEM AND WORKING METHOD

Industrial filling systems used in the pharmaceutical environment typically consist of filling devices coupled with weighing scales. Depending on the type of product handled by the machine, containers such as bottles, vials, or syringes are moved through a conveyor system under the pumps.

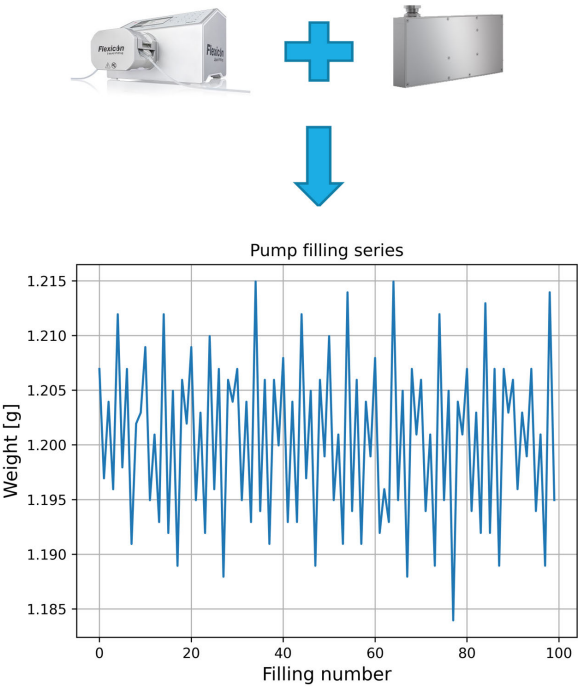

FIGURE 2. Time series produced by a filling system.

These containers are filled with the specific product and then weighed to check the volume dispensed during the process. As shown in Figure 2, when these two devices are used together in a production process, they generate a time series where each observation represents a dispensed volume.

Typically, time series are composed of a predictable and an unpredictable part. This can be observed by calculating the auto-correlation graph after a production process, as shown in Figure 3. The graph indicates a strong correlation between the volumes dispensed during the process time, suggesting the possibility of improving the system's accuracy by applying prediction techniques. The results of these techniques can be used to compensate for subsequent volumes dispensed by the filling system itself. In this study, the dosing system, comprising the peristaltic pump and its associated controller, is explicitly treated as a black box. The approach adopted does not rely on access to the internal model or algorithms of the controller. Instead, the focus is on utilizing the input and output information provided by the system. The pump controller exposes a set of well-defined API software interfaces, carefully designed to prevent improper usage of the system. Through strict adherence to these APIs, it is guaranteed that any data or commands sent to the controller are within the prescribed operational limits. This mechanism adds a layer of stability, protecting the dosing process from potential errors or inaccuracies that might arise from incorrect operations. By treating the system as a black box, the proposed method gains the advantage of potential applicability to diverse control devices, distinct from the specific one presented in the study. The utilization of the ARIMA model enables to capture predictable patterns within

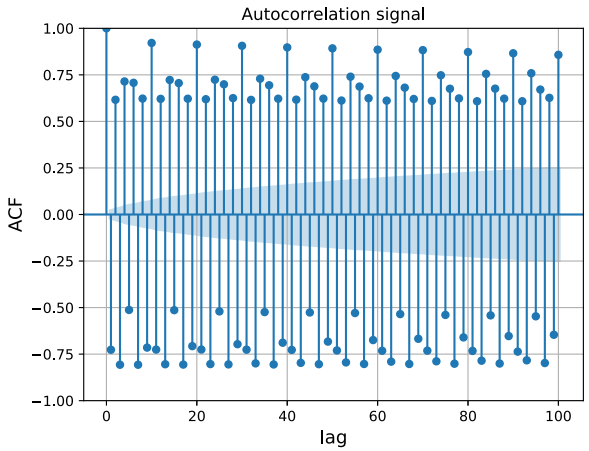

FIGURE 3. Auto-correlation of a time series calculated over a production process.

the time series data and generate accurate predictions for future volumes.

The study presented in this article is organized into four main steps. First, a data gathering campaign is performed to retrieve time series in different working scenarios, which is fundamental for the second phase where these datasets are studied to better understand and control the system's behavior. The third step focuses on evaluating and proposing an ARIMA model to be applied, which is finally tested in a real setup in the fourth and final phase.

All experiments in this study were conducted using a dedicated workstation designed to accelerate the data collection process and simulate different conditions. The workstation replicated the filling process described earlier, which occurs in real industrial machines. Therefore, the most important equipment involved in the process was the same as that normally installed in industrial applications.

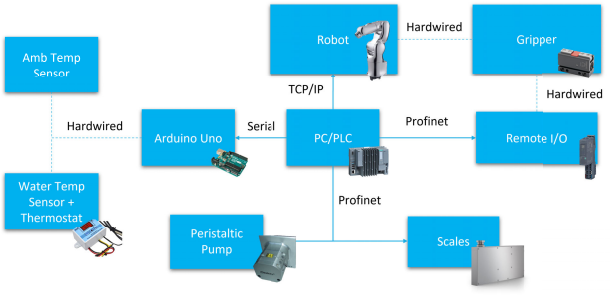

FIGURE 4. Workstation equipment composition.

In the following paragraphs, referring to Figure 4, the components of the workstation will be explained in detail from both the hardware and software perspectives.

B. HARDWARE SETUP

As mentioned in Section II-A, the workstation used for data collection consists of several devices commonly employed in real industrial scenarios. Specifically, a Flexicon PD12 peristaltic pump (PP) system controlled by a Flexicon MC100 control unit [23] (Watson-Marlow Flexicon, Ringsted, Denmark) was utilized for filling.

Two pieces of 1.2 mm ID pump tubing (Flexicon Accusil™) were connected via a Y-connector, both pre- and post-pump. Another two pieces of the same pump tubing were used to complete the dosing circuit: one connected to a liquid reservoir and the other to a 1.6 mm ID nozzle, with a total piping length of approximately 2 m. According to the PP manufacturer [24], this setup can handle volumes in the range of [1.0 - 2.0] ml. For all subsequent tests, a volume of 1.2 ml was chosen. A simplified representation of the pump tubing setup is shown in Figure 5.

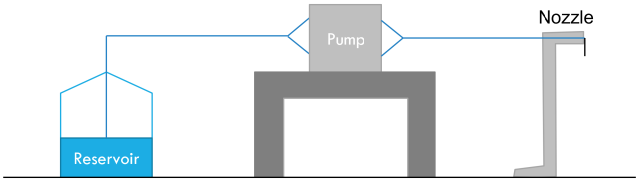

FIGURE 5. Pump tubing setup.

Purified water, filtered by a Milli-Q® Advantage A10 equipped with a Millipak® Express 40 filter, was used in each experiment. The filling experiments, unless stated otherwise, employed the PP at a pre-set velocity of 600 rpm and an acceleration of 200 rpm/s. The suck-back (SB) was set to 1. For the Flexicon PP, the acceleration settings range from 1 to 200 rpm/s, and the SB settings range from 1 to 10. Before each experiment, a purging session was performed to remove air from the piping by activating the PP for a few seconds. Following this procedure, the PP was calibrated to a specific fill volume according to the executed experiment. To measure the dispensed volume, a Wipotec SL-M 250/300 (Wipotec, Kaiserslautern, Germany) high-precision weighing scale (WS) installed in a Modular Multilane System (MMS) was used. The WS was equipped with an Active Vibration Compensation (AVC) sensor to minimize noise, and a CAN-Fieldbus-Interface (CFI) gateway module was employed for Profinet communication. The movement of containers between the PP system and the WS was facilitated by a Denso VS-050S2 (Denso, Kariya, Aichi, Japan) robot, which meets the stringent requirements of the pharmaceutical and medical industry. A Gimatic MPXM gripper (Gimatic, Brescia, Italy) served as the hand-effector for container handling. The entire system was controlled by a Siemens ET 200SP Open Controller (Siemens, Munich, Germany), which combines the functionality of a PLC with a Windows PC-based platform. During the process, environmental and product temperatures were collected via serial communication using sensors placed in the working area and inside the reservoir. The product sensor was coupled with a thermostat to regulate the product temperature, as needed.

C. SOFTWARE SETUP

The software architecture consists of two main components, both handled by the Siemens Open Controller:

1) **PLC-side**: This component manages the PP, WS, robot, and gripper.
2) **PC-side**: This component executes a Python application responsible for the forecasting process. It gathers data from the PLC and calculates the forthcoming filling.

More specifically, the PLC controls the PP, robot, and WS to replicate a standard filling process. It commands the robot to weigh a container, fill it, and measures the dispensed volume. To simulate an infinite flow of containers, a loop is applied in the process, as follows:

1) The robot tares the container by placing it on the WS.
2) The robot positions the container under the needle and initiates the dispense command on the PP.
3) The robot moves the container back to the WS and measures its net weight.
4) If the container is not yet full, the process returns to step 1. Otherwise, it proceeds to step 5.
5) The robot empties the container into the same tank from which the pump draws the product, then returns to the first step.

Depending on the experiment, the PC can execute a Python application that receives the previously dispensed volumes. Once a sufficient number of fillings, known as the training window (TW), have been collected, the application applies the ARIMA model with different configurations. The ARIMA model is implemented using the `Statsmodels` Python package [25], which calculates and returns the forecasted volumes. These volumes are transmitted to the PLC, which adjusts the quantity dispensed by the PP using the appropriate function on the PP control unit. This compensation is calculated to reduce the error, which is the difference between the desired target volume and the actual volume dispensed by the filling device. Communication between the PLC and PC is established using OPC-UA, as illustrated in Figure 6.

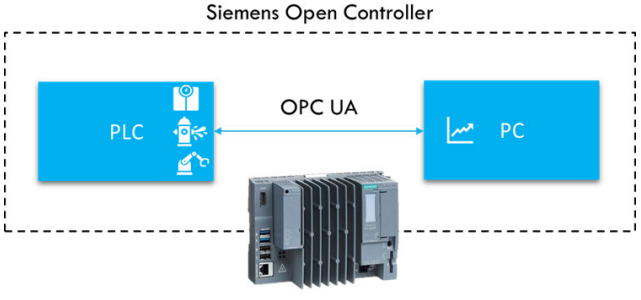

FIGURE 6. Communication protocol used to exchange data between the PLC (responsible for handling the WS, PP, and robot) and PC (responsible for the forecasting process) components in the Siemens Open Controller.

III. EXPERIMENTS AND DATA ANALYSIS

The experiments conducted in this study can be categorized into two main types:

- The first group focused on understanding the physical phenomena that influence pump accuracy, aiming to identify the optimal dosing conditions for the PP. In this phase, no compensations were performed.
- The second group aimed to improve dosing accuracy by using the ARIMA model as a prediction method and applying compensation at each dispense operation. Throughout this experimental process, numerous tests have been conducted to ensure that the dosing system remains stable. Particular care was taken to analyze the system's behavior under various conditions, thereby affirming its coherent and reliable behavior.

A. PUMP DOSING BEHAVIOR

As mentioned briefly in the previous section, the first series of experiments aimed to understand the phenomena occurring during the operation of dosing devices, which determine their accuracy. Thousands of doses were collected by running the system uninterrupted for several days, following the steps outlined in Section II-C. Each batch started with the replacement of the two pieces of tubes within the Y-connector and the calibration of the pump to a target volume of 1.2 ml. Additionally, the filling process was performed without controlling temperature stability. A total of 10 different batches were conducted, each consisting of approximately 20,000 dispenses.

When plotting the amount of water dosed against the filling number, the various runs exhibit similar trends, as shown in Figure 7. Several features can be observed from the filling data:

1) A seasonal component with a time period of approximately 24 hours.
2) Rapid and small fluctuations occurring over one or more fillings.
3) A relatively slow average decay trend.

In Figure 7a, a linear fit of the decay reveals a slope of about −7e-6 g/filling, indicating a loss of 7 mg every 1000 fillings. This behavior is known [26] and find an explanation on the continuous wearing of the tube due to the action of the pump rollers. Figure 7b shows the curve resulting from subtracting the best-fit line (a second-order polynomial) from the data. It represents an oscillating signal superimposed on the mean decay trend, which correlates perfectly with the temperature reading of the water in the tank. The temperature variation, around 3 degrees, was caused by the air conditioning system in the building where the filling setup was located. The visible lag in Figure 7c between the ambient temperature and the temperature of the liquid in the tank can be attributed to the thermal inertia of the water, resulting in a delay in reaching thermal equilibrium. The corresponding variation in dispensed weight is approximately 20 mg. The correlation between water temperature and

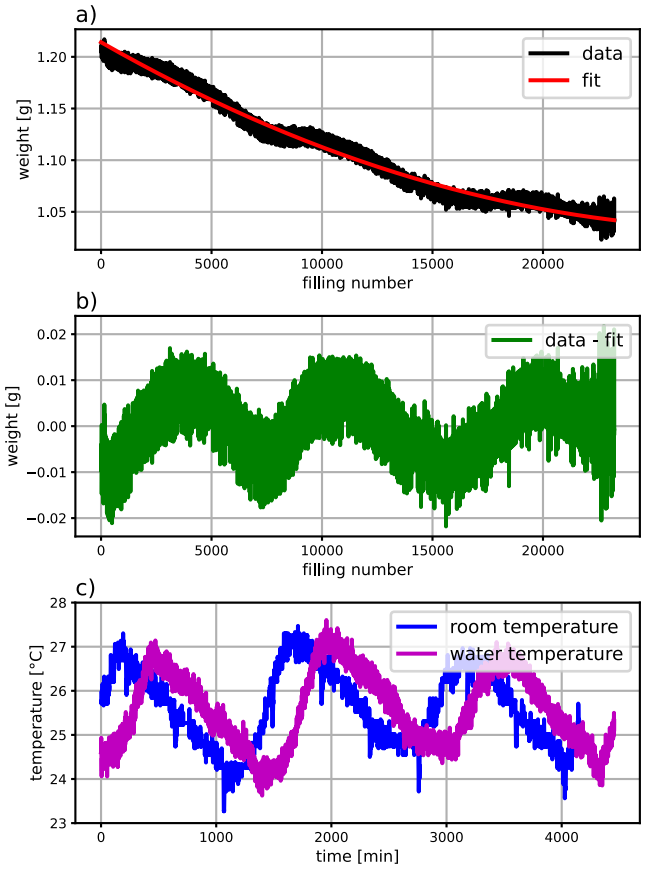

FIGURE 7. a) Filling data with second order polynomial best-fit line. b) Subtraction of best-fit line from the data. c) Room/water temperature fluctuations caused by air conditioning system of the building.

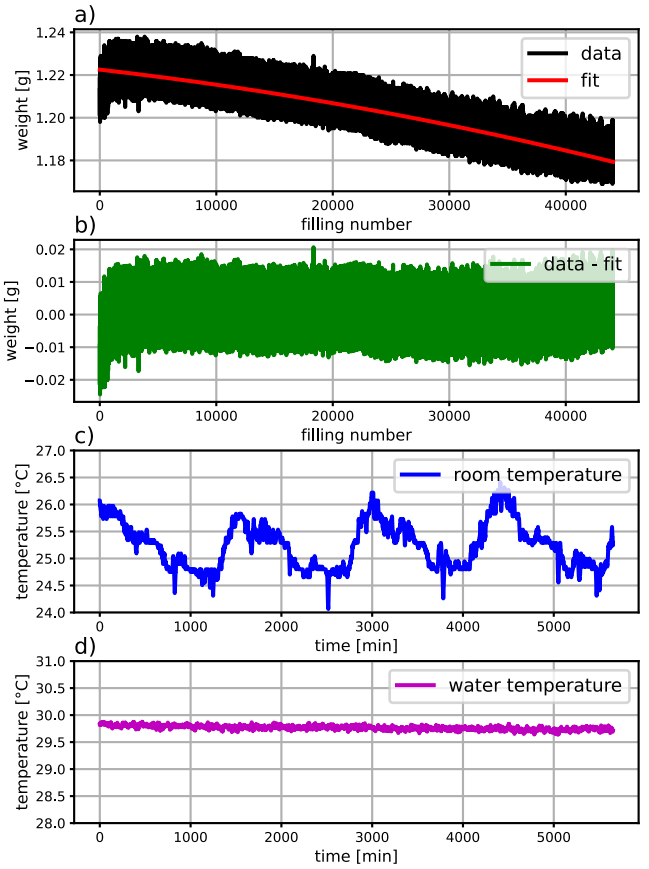

FIGURE 8. a) Filling data with second order polynomial best-fit line. b) Subtraction of best-fit line from the data. c) Room temperature fluctuations caused by air conditioning system of the building. d) Water tank temperature kept constant by using a thermostat.

dispensed volumes is positive, indicating that higher water temperatures correspond to higher dispensed volumes.

In a subsequent experiment, the water temperature in the tank was maintained constant at around 30.0 ± 0.1°C using the thermostat mentioned in Section II-B. The new scenario, plotted in Figure 8, shows that the seasonal component in the filling data disappears, indicating that only variations in water temperature, not air temperature, are responsible for this phenomenon.

Further investigations were conducted to understand the physical mechanisms underlying the relationship between product temperature and dispensed volume. The following three temperature-related factors were considered:

1) Density variation of water.
2) Thermal expansion of the pump tube.
3) Elasticity of the dosing tube.

The subsequent sections provide further details to evaluate the relative significance of each factor and determine if they are sufficient to explain the observed temperature sensitivity.

1) DENSITY VARIATION OF WATER

A simple calculation reveals that the observed range of approximately 20 mg in filled weight cannot be solely explained by the variation in water density. According to [27], the density of water at the two extreme temperatures observed during the experiment, 24°C and 27°C, is approximately 0.99730 g/ml and 0.99652 g/ml, respectively, at a normal pressure of 1 atm. Assuming the dosed volume V_d remains constant at 1.2 ml, the resulting mass variation is:

$$\Delta m = V_d \times \Delta p \approx 0.8 \text{ mg} \tag{1}$$

Not only is this value significantly lower than the observed 20 mg, but it would also imply a negative correlation with temperature. According to this calculation, higher temperatures should result in lower filled weights.

2) THERMAL EXPANSION OF PUMP TUBE

The tube used in the system is made of Flexicon Accusil™, a type of silicone called Polydimethylsiloxane (PDMS). Its cross-section geometry is illustrated in Figure 9. When the tube undergoes thermal expansion, its internal surface area increases, resulting in a larger volume of water that can be accommodated per unit length. Both analytical and numerical calculations have been conducted, with the latter performed using the COMSOL Multiphysics™ [28] software package. The two methods yield similar results, indicating a weight

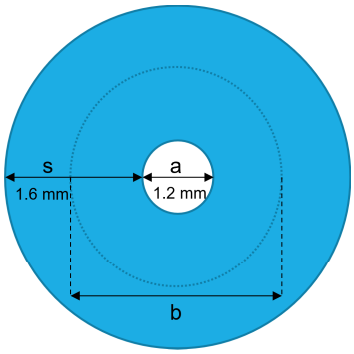

FIGURE 9. Cross-section of the Flexicon Accusil™tube.

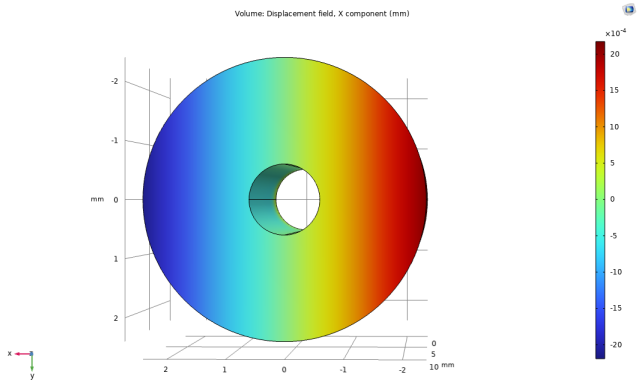

FIGURE 10. Von Mises stress of the tube section after thermal expansion. Only the *x* component of the stress is depicted on the plot.

variation of 2.2 mg. This effect exhibits a positive correlation with temperature variation, but it accounts for only around 10-15% of the total observed mass variation.

a: ANALYTICAL CALCULATION

In the analytical calculation, small temperature variations denoted as dT are considered. The relative change in length $\frac{dl}{l}$ is given by the thermal expansion coefficient α, which for PDMS is 3×10^{-4} K^{-1} [29], [30]:

$$\frac{dl}{l} = \alpha dT. \tag{2}$$

To determine the length variation of the internal diameter a, changes in both the circumference of diameter b and the tube thickness s are taken into account. From Figure 9, $b = a + s$, and therefore:

$$da = db - ds. \tag{3}$$

Substituting this into the equation:

$$\frac{da}{a} = \frac{db - ds}{b - s} = \frac{\alpha b dT - \alpha s dT}{b - s} = \alpha dT. \tag{4}$$

Since the internal section S of the tube is proportional to a^2 and assuming a constant density of water, the relative variation of weight is given by:

$$\frac{dm}{m} = \frac{dS}{S} = 2\frac{da}{a} = 2\alpha dT. \tag{5}$$

Substituting the given values $dT = 3$°C and $m = 1.2$ g into the formula, the resulting mass variation is:

$$dm = 2.2 \text{ mg}. \tag{6}$$

b: NUMERICAL CALCULATION

Numeric calculations were performed using the COMSOL Multiphysics™software. The study utilized the exact geometry shown in Figure 9, with the PDMS material selected (the thermal expansion coefficient was corrected from $9K^{-1}$ to $3K^{-1}$ according to [29] and [30]), available in the COMSOL material database. The Thermal Expansion model was chosen to represent the physics. The environmental temperature and the external surface of the tube were maintained at 27°C, while the temperature of the internal part was raised from 24°C to 27°C. The simulation output can be visualized through von Mises stress, as shown in Figure 10. Due to the symmetry of the tube, the magnitude of the stress depends solely on the distance from the center of the cylinder.

The mass variation resulting from the increase in internal diameter is the same as the previous one within 0.1 mg. The combined effect of thermal expansion (2.2 mg) and the change in water density (−0.8 mg) accounts for approximately 7% of the total observed mass change, which is around 1.4 mg.

3) ELASTICITY OF DOSING TUBE

To observe the trend of the dosed volume as a function of controlled changes in water temperature, a short run was performed by varying the temperature. Specifically, the temperature was raised from 28°C to 36°C in 2°C increments. Continuous dosing was carried out for approximately 30 minutes at each temperature. The results are shown in Figure 11.

The step-wise temperature variation shown in Figure 11b is clearly reflected in the dosed volume shown in Figure 11a. The increase in dosed volume decreases as the temperature rises. The first step has an amplitude of approximately 20 mg, the second of 12 mg, the third of 7 mg, and the fourth of 4 mg. This trend does not align with a simple thermal expansion effect of the tube, which would have resulted in quasi-constant steps.

Subsequent tests have revealed that these variations are mainly due to the relaxation time of the tube's geometry between two successive deformations caused by the pump rollers. When dosing at the maximum speed achievable by the pump, i.e., 600 rpm, the tube cannot reach its rest position before the next roller deforms it again. As the temperature increases, the tube becomes more elastic, allowing it to relax completely after each deformation.

Three experiments were conducted at different pump speeds: 600 rpm, 300 rpm, and 100 rpm, to emphasize this phenomenon. Each dosing experiment lasted approximately 30 minutes at a temperature of 26°C, after which the temperature was increased to 30°C, and dosing continued for another 30 minutes.

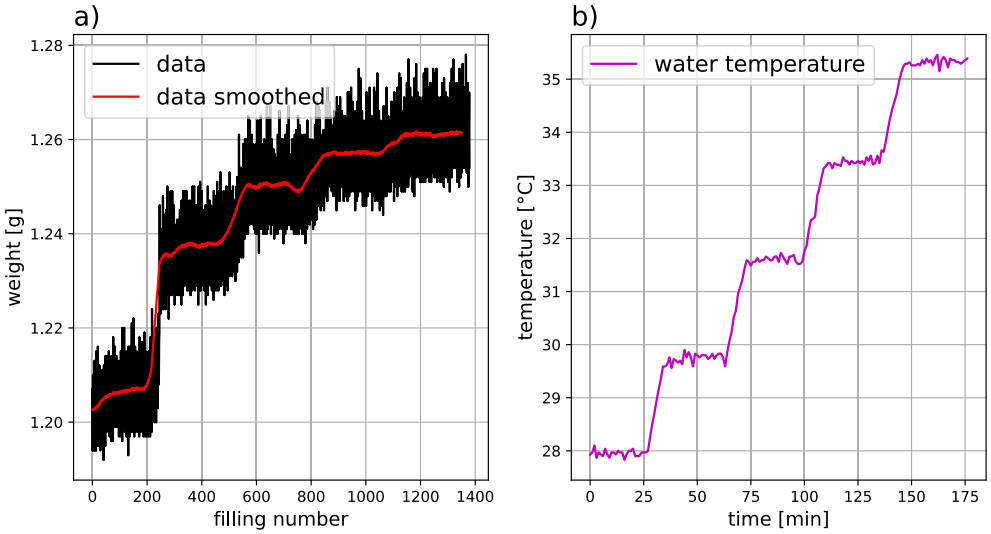

FIGURE 11. a) Filling data for different water temperatures. The red line represents a smoothing of the data using a 30-point window. b) Stepwise temperature variation from 28 to 36°C.

Figure 12a clearly shows that at a pump speed of 600 rpm, a temperature increase of 4°C results in a step of approximately 30 mg in the dosages.

By reducing the speed to 300 rpm (Figure 12b) and 100 rpm (Figure 12c), the residual step is on the order of a few milligrams, which corresponds to the overall contribution resulting from the thermal expansion effect of the tube and the change in water density. These results demonstrate that changing the temperature of the dispensed product alters the elasticity of the tube. Moreover, this phenomenon explains 93% of the dosed mass variation due to temperature change, as the remaining elements analyzed in the previous paragraphs account for the remaining variation.

4) CONCLUSION

In conclusion, the results obtained in this initial part of the study demonstrate that changing the temperature of the dispensed product causes a variation in filling accuracy primarily due to the combination of three major phenomena, listed in order of relevance:

1) **Elasticity of the dosing tube**: which is influenced by the temperature increase of the product, making the tube progressively more elastic. This allows the tube to relax completely after each deformation caused by the pump rollers, as explained in Section III-A3. This factor is closely related to the pump rotation speed as well. Slower pump rotation results in better alignment between the displaced volume and the actual pipe capacity since the tube has more time to relax after each deformation.
2) **Thermal expansion of the pump tube**: which leads to a mass variation in the dispensed product of approximately 10-15% of the total observed mass variation, as discussed in Section III-A2.
3) **Density variation of water**: which causes a slight decrease in the dosed volume per unit, as shown in Section III-A1.

To ensure system control and achieve stable filling accuracy, it is important to maintain a fixed product temperature and pump rotation speed at specific values.

Finally, by controlling the temperature and conducting time-limited runs to minimize the influence of tube consumption, it was possible to determine the accuracy value of the dosing device. For the volumes considered in the experimental phase, the accuracy was found to be less than $\pm 1\%$, in accordance with the manufacturer's statement [1].

B. ADCS THROUGH ARIMA MODEL

In the following sections, a new method is proposed that is capable of improving the accuracy of the pump beyond its inherent limits. Specifically, the aim of the second series of experiments was to develop and test the ADCS by applying an ARIMA model [18] to forecast future fillings and implementing a compensatory mechanism. This was made possible through the PLC-PC interaction described in Section II-C.

In time series analysis, an ARIMA model is a generalization of an Autoregressive Moving Average (ARMA) model. Both models are fitted to time series data to understand the data better or predict future points in the series (forecasting). ARIMA models are applied when the mean trend of the data is not constant, meaning that the data is not stationary. When a periodic behavior (seasonality) is present in addition to the mean trend, seasonal differencing can be applied to eliminate this component and work with only the residual noisy part of the data. The AR part of ARIMA models the evolving variable of interest as a linear combination of its past values. The MA part, similar to autoregression, is a linear combination of past white-noise error terms.

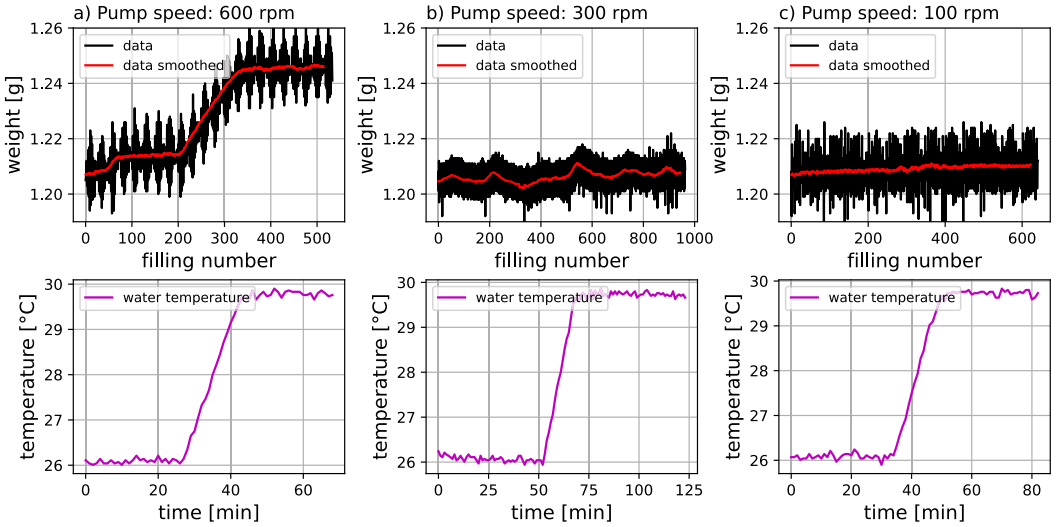

FIGURE 12. Filling data with pump speed set to 600 rpm (a) , 300 rpm (b), 100 rpm (c), and temperature ranging from 26 to 30°C.

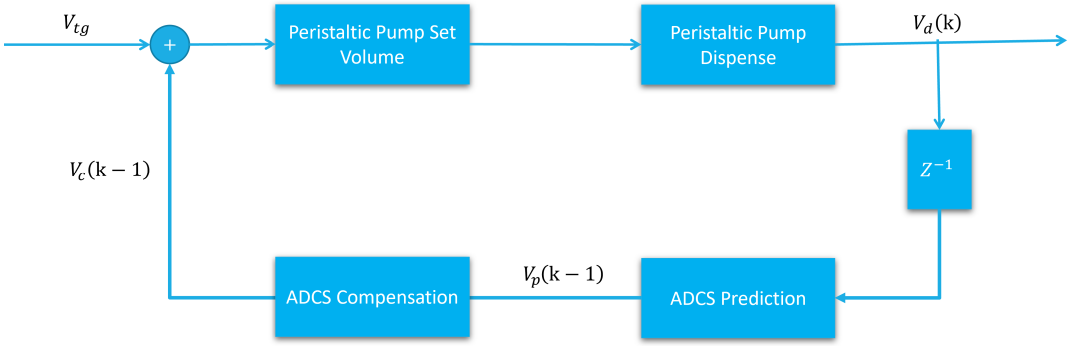

FIGURE 13. Logic representation of the implemented ADCS.

The I (integrated) indicates that the original time series has been differenced one or multiple times to remove the mean trend. The purpose of each of these features is to make the model fit the data as well as possible. Non-seasonal ARIMA models are typically denoted as ARIMA(p, d, q), where arguments p, d, and q are non-negative integers. The parameter p represents the order (number of time lags) of the autoregressive model, d is the degree of differencing, and q is the order of the moving-average model. These three inputs determine the effectiveness of the forecasting results. In the first phase of the study, specific tests were conducted to identify the best values for these parameters. In the second phase, two different adaptive approaches based on the ARIMA model were evaluated in real-time to improve accuracy performance. A schematic representation of the implemented control system is shown in Figure 13, where V_{tg} represents the target volume, V_d is the dispensed volume, V_p is the predicted volume, and V_c is the compensation amount to be added for the forthcoming filling. These approaches involved dynamically adjusting the next filling volume based on the predicted dosed volume V_p. The adaptability of the system relies on the absence of prior knowledge regarding the model governing the dosing system. As the PP continuously doses, the temporal behavior of the compensated volumes V_d is kept monitored, and the compensation amount V_c is adjusted accordingly to optimize dosing accuracy. By continuously analyzing the time series data and predicting the next dosed volume, the system can calculate the compensation and incorporate it as an input to the pump controller. This adjustment mechanism ensures adaptation to the uncertain and potentially time-varying behavior of the dosing system, thus improving accuracy and compensating for the forthcoming filling.

1) ARIMA PARAMETER EVALUATION

As discussed in Section III-A, the dosing trends consist of three main components: an average decay due to tube deterioration, a seasonal component with a 24-hour period caused by temperature variations, and rapid small fluctuations over one or more fillings.

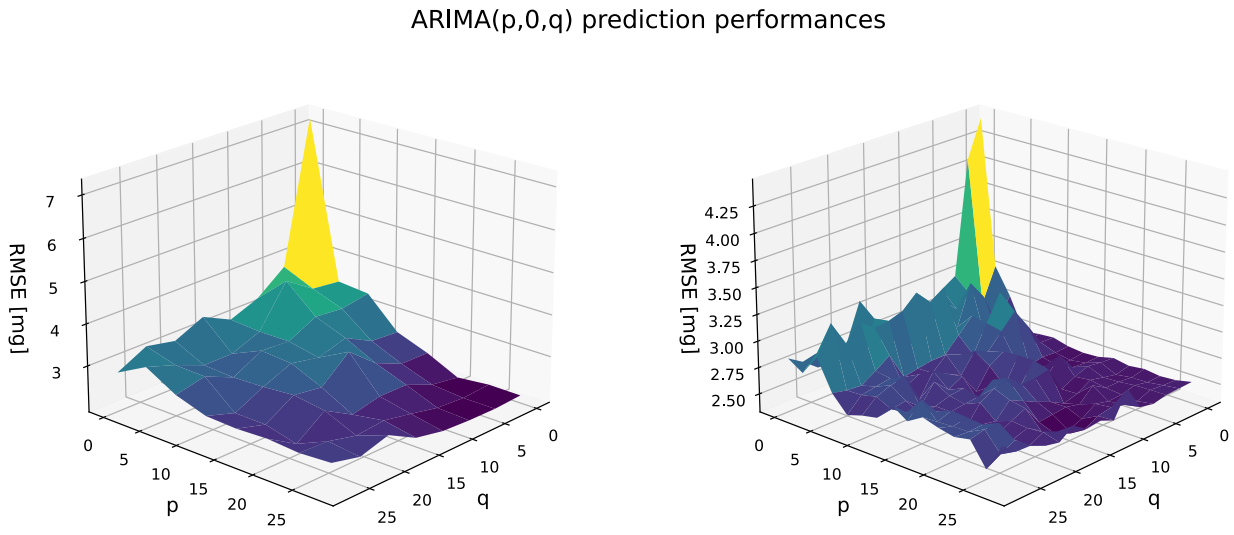

FIGURE 14. ARIMA(p, 0, q) prediction performances measured for different (p, q) pairs and averaged over different runs. Performances are expressed in terms of RMSE between predicted and actual weight values.

The decay due to tube deterioration and the seasonal component can affect the stationarity of the trend. The degree of differencing (parameter d) can be used to make the signal stationary and improve the forecasting performance of the ARIMA model. However, based on the previous analysis, the tube consumption phenomenon was found to have a negligible effect, causing only a minimal loss of a few milligrams per 1000 fillings. The seasonal component can also be neglected by setting the temperature to a constant value, as was done in the experiments. Therefore, it can be assumed that the filling trend, within a time-limited range, can be considered stationary without loss of generality, and differencing is not necessary.

Several experiments confirmed that the argument d had no significant effects on the forecasting performance. However, dedicated tests were conducted to determine the optimal values for the remaining two parameters.

Using the datasets collected in Section III-A, where the pump was calibrated at the beginning of each process, pairs (p, q) with p and q ranging from 0 to 28 were evaluated, resulting in a total of 400 pairs. The performance of each model was measured using Root Mean Squared Error (RMSE), a commonly used metric for evaluating prediction quality. RMSE measures the average squared difference between the predicted and observed values and is expressed as:

$$RMSE = \sqrt{\frac{1}{n}\sum_{i=1}^{n}(P_i - O_i)^2}, \tag{7}$$

where O_i are the observed fill volumes, P_i the predicted fill volumes and n the number of observations available for the analysis.

RMSE values were collected by repeating the fit of a given model on different subsets of the entire datasets shifted by five forward weights at a time, until a cutoff value in the series, set at the 1000-th dose, was reached. To train the model's parameters, datasets with different lengths, known as training windows (TW), were considered, ranging from 100 to 300 points. These points were extracted from the available series. The selection of the TW is crucial as it greatly influences the model's accuracy and its ability to capture underlying patterns in the data. The TW size is an important consideration in ARIMA modeling as it significantly affects the model's performance. A larger TW allows the model to capture longer-term dependencies and trends, while a smaller TW focuses more on short-term variations. The chosen range of 100 to 300 points aimed to explore the impact of different TW sizes on the ARIMA model's accuracy specifically for the dosing system under consideration. The goal was to find the optimal balance between capturing relevant dynamics in the data and maintaining the window length as short as possible. During each iteration, the oldest five values in the list were removed, and a new set of five values were inserted at the end of the window to maintain a constant number of points. This process allowed the TW to move through the entire dataset, recalculating the ARIMA prediction for the following dosage.

The results shown in Figure 14 indicate that the best prediction performance is achieved in the high-p and low-q region. This suggests that the model can be reduced to a simple autoregression AR(p).

The reported results are based on tests with a TW size of 100 points, as no significant differences were observed with different window lengths in terms of RMSE.

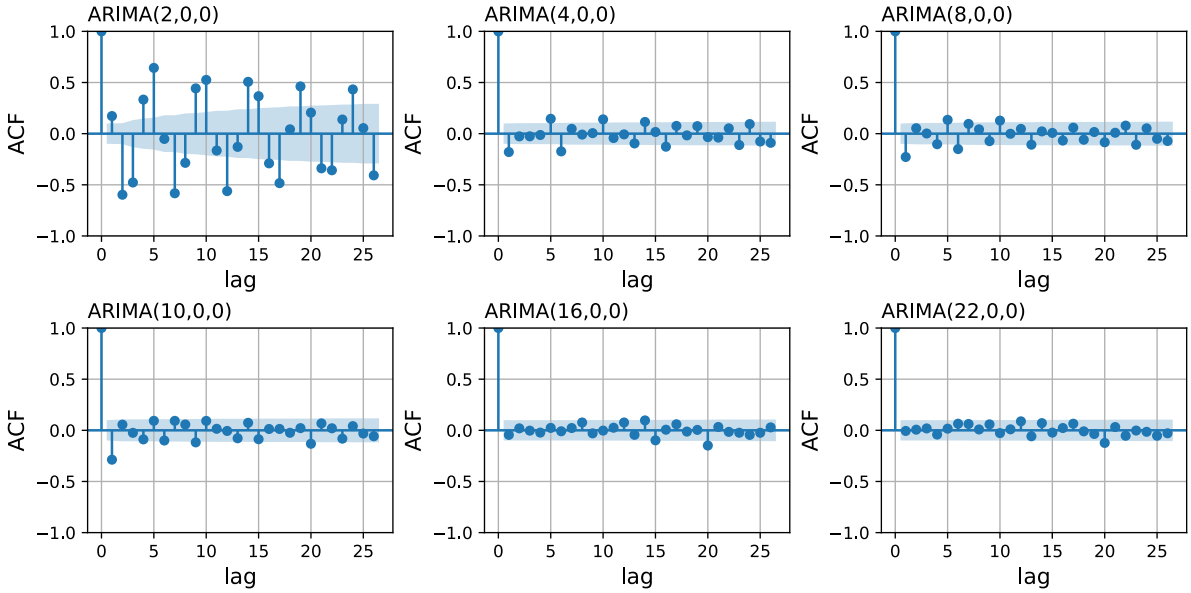

FIGURE 15. Auto-correlation functions of the residuals of ARIMA(p, 0, 0) model.

To assess the prediction process's effectiveness, the autocorrelation of the residuals was calculated for increasing values of p (with q and d set to 0). The residuals represent the differences between the values predicted by the ARIMA model and the corresponding dosed values during the process.

As shown in Figure 15, increasing the autoregressive parameter results in residuals with autocorrelation patterns that resemble white noise more closely. This indicates that as p increases, the model becomes better at forecasting the predictable part of the data. Once p reaches 10 or higher, the auto-correlation patterns become similar. Since further increases in p require higher computation time without significant improvement in terms of auto-correlation, AR(10) was chosen as the optimal parameter for further analysis.

2) ADCS WITH STATIC TRAINING WINDOW

Based on what was discussed in Section III-B1, an AR(10) model was chosen for these experiments. The workstation used was exactly the same as described in Section II-A, the overall control system is depicted in Figure 16, and the logic representation of the ADCS is shown in Figure 13. The experiments conducted in this phase involved calibrating the PP once at the beginning of each process to the target V_{tg}. The water temperature was set to 26°C. In this first algorithm, represented in Figure 17, the main idea is to train the AR model by looking at the last TW dispensed volumes to capture the PP pattern. To improve the filling accuracy, the AR model is used to forecast the next N values. These forecasted measurements are then used to compensate each subsequent dosage of the PP. Once the compensation is completed, new dosages are collected, and the process is repeated. The following steps are performed in more detail:

1) The PP is triggered to dispense the new volume, which is weighted with the WS and inserted into a list called $V_{dispensed}$, as shown in Figure 17a.
2) If the number of measurements collected in $V_{dispensed}$ is less than the designated training window TW, the process repeats from step 1. Otherwise, the next step is performed.
3) Starting from the TW previously observed volumes in $V_{dispensed}$, an AR(10) model is used to forecast the next N fillings, which are stored in the $F_{volumes}[N]$ array, as shown in Figure 17b.
4) For each predicted quantity V_p in $F_{volumes}[N]$:
   a) To increase the accuracy of the PP, volume compensation is performed according to the following formula:

$$V = V_{tg} \cdot \frac{V_{tg}}{V_p} \equiv V_{tg} + V_c = V_{tg} + \frac{V_{tg}}{V_p} \cdot (V_{tg} - V_p). \quad (8)$$

   b) The result is then applied to the PP controller using the *set-volume*(V) primitive to adjust the next dosage according to the forecasted value.
   c) The PP is triggered to dispense the new volume, as shown in Figures 17c, 17d, 17e, and 17f.
5) If the total number of dispensed fillings is sufficient, the process stops; otherwise, the *set-volume*(V_{tg}) primitive is called, $V_{dispensed}$ is cleared, and the process repeats from step 1.

Results calculated after several runs with $TW = 100$, $N = 50$, and reported in Table 2, demonstrate that no performance improvements can be observed. On the contrary,

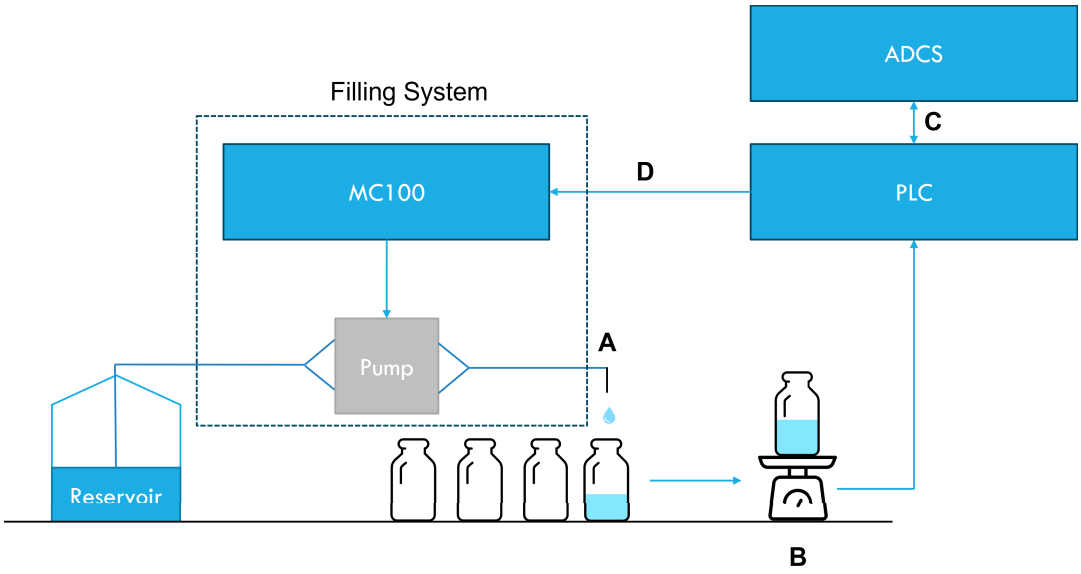

FIGURE 16. Dosing control system. A) The PP is triggered to dispense the volume set into the MC100. B) The filled container is weighted; the weight is registered by the PLC and transmitted to the ADCS. C) the ADCS performs the forecasting process and returns the volume adjustment based on the analysis. D) the PLC sets the adjusted volume into the MC100 by using the *set-volume*() primitive.

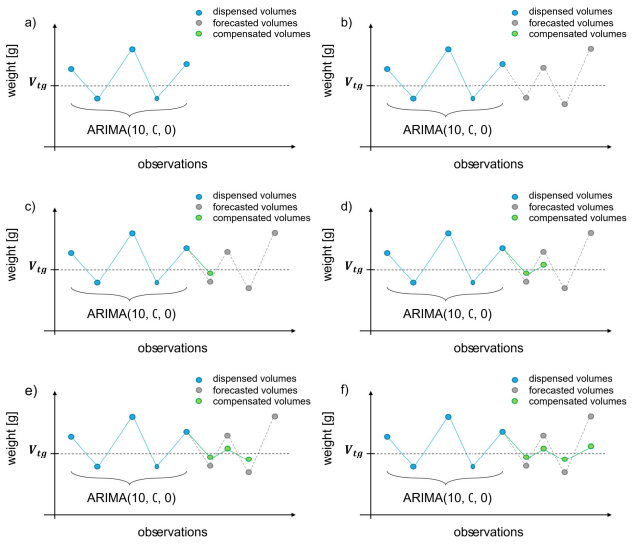

FIGURE 17. ARIMA Adaptive Dosing Control System with Static Training Window representation. a) TW dispensed volumes are collected. b) AR(10) is trained on top of the collected volumes, and the forthcoming N fill volumes are forecasted. c, d, e, f) PP is compensated according to the forecasted volume, and the next fill is triggered, resulting in a dispensed volume closer to V_{tg}.

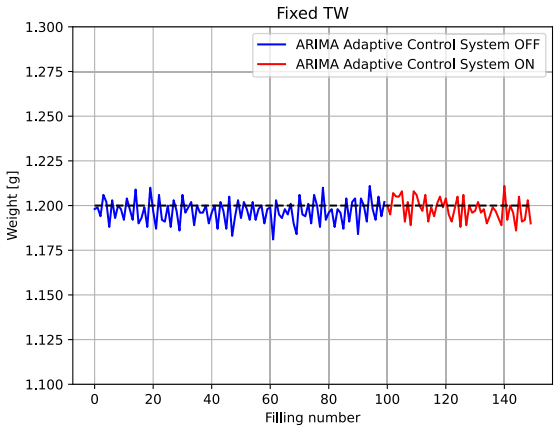

FIGURE 18. Example of a filling process where ADCS with a fixed window, $TW = 100$, $N = 50$, and $V_{tg} = 1.2$ ml, has been applied. The only improvement that can be observed is that the red line is more centered around the target volume, thus resulting in a positive RMSE percentage gain. At the same time, calculations show a worsening in terms of STD gain.

as shown in Table 1, a negative impact on the standard deviation (STD) has been observed, with an average loss of 28.8%. This suggests that the *set-volume*() primitive significantly alters the behavior of the PP, affecting the predictive effectiveness of the AR model. However, applying the ADCS results in a positive average gain of 5.6% with respect to the RMSE, as the system better centers the time series around the target volume. As a reference, an example of a run is reported in Figure 18.

3) ADCS WITH MOVING TRAINING WINDOW

Based on what discussed in Section III-B1, for these experiments an AR(10) model was chosen. The workstation used was exactly the same described in Section II-A, the overall control system is depicted in Figure 16, and the logic representation of the ADCS is shown in Figure 13. The water temperature was set to 26°C. Each experiment began by calibrating the PP to the target V_{tg} at the start of each batch. Subsequently, N consecutive fillings according to the chosen TW were gathered. Once the first TW quantities are collected, the following algorithm is applied (Figure 19a):

1) The AR(10) model is used to forecast the next filling volume, denoted as V_p, based on the previous TW observations (Figure 19b).

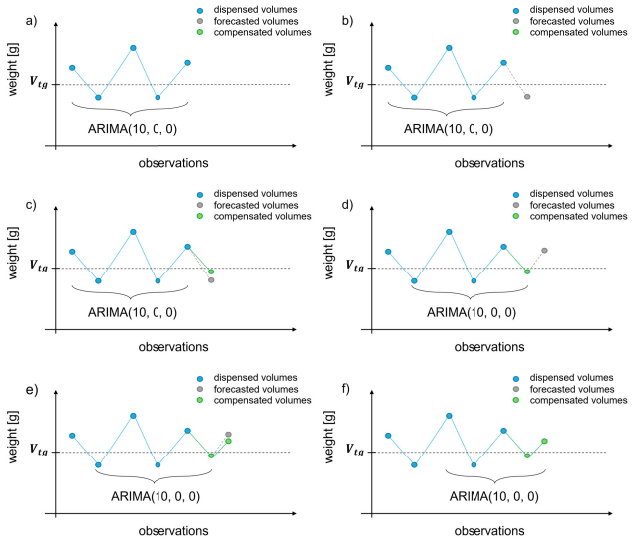

FIGURE 19. ARIMA Adaptive Dosing Control System with Moving Training Window representation. a) TW dispensed volumes are collected. b) ARIMA(10,0,0) is trained on top of the collected volumes and the forthcoming fill is forecasted. c) PP is compensated according to the forecasted volume and the next fill is triggered resulting in a dispensed volume closer to the V_{tg}. d) The TW is moved to consider the last compensated volume and ARIMA(10,0,0) is trained producing another forecast. e) PP is compensated according to the forecasted volume and the next fill is triggered resulting in a dispensed volume closer to the V_{tg}. f) The TW is moved to consider the last compensated volume and ARIMA(10,0,0) is trained.

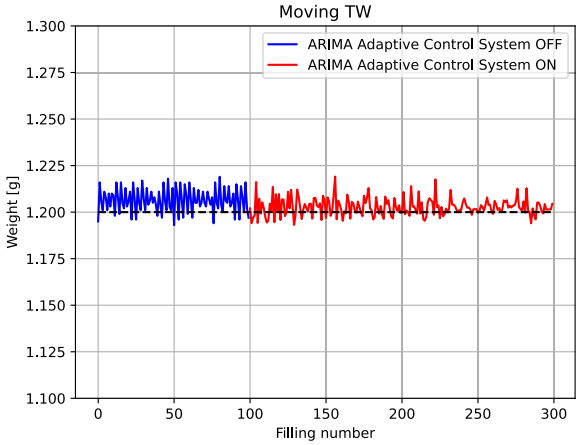

FIGURE 20. Example of a filling process where ADCS with a moving window, $TW = 100$, and $V_{tg} = 1.2$ ml was applied. In this case, both the STD and RMSE percentage gains show positive improvements, and it is clearly visible as the red line is better centered and more compact around V_{tg}.

2) To improve the accuracy of the PP, a compensation is performed according to the Formula 8.
3) The resulting volume is then applied to the PP controller using the *set-volume*() primitive to adjust the next filling based on the forecasted value.
4) The PP is triggered to dispense the new dosage (Figure 19c). To keep the *TW* length unchanged, at each iteration, the oldest value in the list is removed and the new compensated value dispensed is inserted at the end of the window (Figure 19d).
5) If the total number of dispensed fillings is sufficient, the process stops. Otherwise, the process is repeated from step 1.

TABLE 1. Precision gain of the pump using STD as the evaluation metric. The first column indicates the target volume used in the experiment. The second column specifies the approach used for compensation: moving or fixed training window. The third (fourth) column shows the STD of the filling series when ADCS is turned off (on). The last column represents the percentage gain in STD obtained when ADCS is activated. A positive gain indicates an increase in pump accuracy. All values are averaged over multiple runs.

Target [mg]	TW	RMSE - ADCS Off [mg]	RMSE - ADCS On [mg]	Gain [%]
1200	Moving	5.7	4.5	19.5
1200	Fixed	5.5	6.9	-28.8

TABLE 2. Precision gain of the pump using RMSE as the evaluation metric (the error is relative to the target volume). Please refer to Table 1 for a description of the column contents.

Target [mg]	TW	RMSE - ADCS Off [mg]	RMSE - ADCS On [mg]	Gain [%]
1200	Moving	7.3	5.0	29.4
1200	Fixed	7.7	7.0	5.6

In this case, better results are achieved. As reported in Tables 1 and 2, both the percentage gains in STD and RMSE were positive, with values of 19.5% and 29.4% respectively. This indicates that the ADCS with a moving training window not only brings the mean value closer to the target volume but also reduces the width of the value distribution around the mean. As a reference, an example run is shown in Figure 20.

IV. CONCLUSION

In this paper, a real industrial dosing system was analysed with two objectives: i) studying the relationship between product temperature and dosing accuracy and ii) using an adaptive control system to increase the accuracy performance. Firstly, a thorough investigation revealed that alterations in the elastic properties of the tube material due to the temperature of the product is one critical phenomena that directly impact the dosed volume. The results have highlighted the significance of considering temperature effects for achieving precise dosing in real production lines, particularly in pharmaceutical applications. By understanding the pivotal role of tube deformation in influencing dosed volumes, valuable implications have been provided for optimizing dosing accuracy in various industrial dosing setups. In pursuit of the second objective, an adaptive control system based on the AR model was proposed to enhance accuracy performance even under optimal working conditions, where temperature has been stabilized. Two different approaches were introduced to implement the prediction system called ADCS: one employing a static training window to forecast the forthcoming volumes and another utilizing a moving training window to forecast one volume at a time. The latter approach has shown good results, yielding a remarkable 30% increase in pump dosing accuracy. This strategy, treating the system as a black box, provides the

advantage of potential applicability to diverse dosing setups beyond the specific one studied, making it adaptable for various industrial applications.

As future work, exploration will be conducted on the use of machine learning (ML) techniques for time series prediction in comparison to the ARIMA model. While ARIMA has proven to be a reliable and simple approach for the current task, there may be other ML methods, such as Recurrent Neural Networks (RNNs) and Transformers, which have shown promising results in time series prediction tasks, despite their higher model complexity. These ML models are capable of capturing non-linear relationships and patterns in the data, which may be difficult to identify using traditional statistical methods like ARIMA. Overall, the integration of ML techniques may lead to improved accuracy and efficiency in time series prediction tasks. Through these future works, comprehensive evaluations will be conducted on different prediction techniques and their applicability to this specific domain, further enhancing dosing precision and advancing the field of precision filling technology in industrial applications.

ACKNOWLEDGMENT

The authors would like to thank Pharma Integration [21] in the persons of Claudio Bechini and Cinzia Butini for providing them with the opportunity to use the necessary equipment to conduct our experiments. Their generous contribution has been crucial to the success of our work. They also like to thank Francesco Bernabei for his contribution to the initial phase of our study through his thesis work. Without their valuable support, they would not have been able to achieve the results presented in this paper.

REFERENCES

[1] P. Lambert and F. Joergensen, "Accurate dispensing of biopharmaceuticals," *World Pumps*, vol. 2008, no. 498, pp. 22–24, Mar. 2008.

[2] T. Dreckmann, J. Boeuf, I.-S. Ludwig, J. Lümkemann, and J. Huwyler, "Low volume aseptic filling: Impact of pump systems on shear stress," *Eur. J. Pharmaceutics Biopharmaceutics*, vol. 147, pp. 10–18, Feb. 2020. [Online]. Available: https://www.sciencedirect.com/science/article/pii/S0939641119313177

[3] J. Klespitz and L. Kovács, "Peristaltic pumps—A review on working and control possibilities," in *Proc. IEEE 12th Int. Symp. Appl. Mach. Intell. Informat. (SAMI)*, Jan. 2014, pp. 191–194.

[4] W. Shieu, D. Lamar, O. B. Stauch, and Y.-F. Maa, "Filling of high-concentration monoclonal antibody formulations: Investigating underlying mechanisms that affect precision of low-volume fill by peristaltic pump," *PDA J. Pharmaceutical Sci. Technol.*, vol. 70, no. 2, pp. 143–156, Mar. 2016. [Online]. Available: https://journal.pda.org/content/70/2/143

[5] S. M. Wu and J. Ni, "Precision machining without Precise Machinery," *CIRP Ann.*, vol. 38, no. 1, pp. 533–536, 1989. [Online]. Available: https://www.sciencedirect.com/science/article/pii/S0007850607627620

[6] X. Wang, Q. Bi, L. Zhu, and H. Ding, "Improved forecasting compensatory control to guarantee the remaining wall thickness for pocket milling of a large thin-walled part," *Int. J. Adv. Manuf. Technol.*, vol. 94, nos. 5–8, pp. 1677–1688, Feb. 2018.

[7] X. Wang, Q. Bi, and L. Zhu, "Improved forecasting compensatory control through Kalman filtering," *Proc. CIRP*, vol. 56, pp. 349–353, Dec. 2016. [Online]. Available: https://www.sciencedirect.com/science/article/pii/S2212827116310307

[8] K. F. Eman, "A new approach to form accuracy control in machining†," *Int. J. Prod. Res.*, vol. 24, no. 4, pp. 825–838, Jul. 1986, doi: 10.1080/00207548608919769.

[9] P. Turek, J. Jedrzejewski, and W. Modrzycki, "Methods of machine tool error compensation," *J. Mach. Eng.*, vol. 10, no. 4, pp. 5–25, 2010.

[10] L. Yan and W. Huang, "An IC yield enhancement approach by ARMA modeling and dynamic process control," *Int. J. Adv. Manuf. Technol.*, vol. 42, nos. 7–8, pp. 749–756, Jun. 2009.

[11] C. Hu, T. Ou, H. Chang, Y. Zhu, and L. Zhu, "Deep GRU neural network prediction and feedforward compensation for precision multiaxis motion control systems," *IEEE/ASME Trans. Mechatronics*, vol. 25, no. 3, pp. 1377–1388, Jun. 2020.

[12] J. Francis and L. Bian, "Deep learning for distortion prediction in laser-based additive manufacturing using big data," *Manuf. Lett.*, vol. 20, pp. 10–14, Apr. 2019.

[13] H. Liang, L. Chen, Y. Pan, and H.-K. Lam, "Fuzzy-based robust precision consensus tracking for uncertain networked systems with cooperative—Antagonistic interactions," *IEEE Trans. Fuzzy Syst.*, vol. 31, no. 4, pp. 1362–1376, Apr. 2023.

[14] N. Xu, Y. Zhu, R. Yang, X. Chen, and C.-Y. Su, "Adaptive fault-tolerant control for a 2-body point absorber wave energy converter against actuator faults: An iterative learning control approach," *IEEE Trans. Sustain. Energy*, vol. 14, no. 3, pp. 1664–1675, Jul. 2023.

[15] L. Chen, Y. Tan, Y. Zhu, and H.-K. Lam, "Fault reconstruction for continuous-time switched nonlinear systems via adaptive fuzzy observer design," *IEEE Trans. Fuzzy Syst.*, vol. 31, no. 9, pp. 3235–3247, Sep. 2023.

[16] L. Cao, Y. Pan, H. Liang, and T. Huang, "Observer-based dynamic event-triggered control for multiagent systems with time-varying delay," *IEEE Trans. Cybern.*, vol. 53, no. 5, pp. 3376–3387, May 2023.

[17] L. Chen, Y. Zhu, and C. K. Ahn, "Adaptive neural network-based observer design for switched systems with quantized measurements," *IEEE Trans. Neural Netw. Learn. Syst.*, vol. 34, no. 9, pp. 5897–5910, Sep. 2023.

[18] G. E. Box, G. M. Jenkins, G. C. Reinsel, and G. M. Ljung, *Time Series Analysis: Forecasting and Control*. Hoboken, NJ, USA: Wiley, 2015.

[19] D. Kobiela, D. Krefta, W. Król, and P. Weichbroth, "ARIMA vs LSTM on NASDAQ stock exchange data," *Proc. Comput. Sci.*, vol. 207, pp. 3836–3845, Oct. 2022. [Online]. Available: https://www.sciencedirect.com/science/article/pii/S1877050922013382

[20] P. T. Yamak, L. Yujian, and P. K. Gadosey, "A comparison between ARIMA, LSTM, and GRU for time series forecasting," in *Proc. 2nd Int. Conf. Algorithms, Comput. Artif. Intell.* New York, NY, USA: Association for Computing Machinery, Dec. 2019, pp. 49–55, doi: 10.1145/3377713.3377722.

[21] *Pharma Integration—The Innovative Technology Behind the Facility of the Future*. Accessed: Oct. 10, 2023. [Online]. Available: https://www.pharma-integration.it

[22] European Union. (2022). *The Rules Governing Medicinal Products in the European Union Volume 4 EU Guidelines for Good Manufacturing Practice for Medicinal Products for Human and Veterinary Use—Annex 1 Manufacture of Sterile Medicinal Products*. [Online]. Available: https://health.ec.europa.eu/medicinal-products/eudralex/eudralex-volume-4_en#part

[23] J. Jeppesen. (2009). *MC100 Pump Control Module User's Manual*. [Online]. Available: https://www.wmfts.com/globalassets/literature/m-flexicon-mc100-profibus-en.pdf

[24] F. Jørgensen. (2008). *PD12 OEM Operators Manual*. [Online]. Available: https://archive.org/details/manualzilla-id-6886200

[25] S. Seabold and J. Perktold, "Statsmodels: Econometric and statistical modeling with Python," in *Proc. 9th Python Sci. Conf.*, 2010, pp. 92–96.

[26] A. Peterson, E. Isberg, and A. Schlicht, "Capability of filling systems to dispense micro-doses of liquid pharmaceutical product," *Pharmaceutical Eng.*, vol. 24, no. 4, p. 7, Jul. 2007.

[27] E. W. Lemmon, I. H. Bell, M. L. Huberm, and M. O. McLinden, "Thermophysical properties of fluid systems," in *NIST Chemistry Webbook—NIST Standard Reference Database 69*, P. Linstrom and W. Mallardy, Eds. Gaithersburg, MD, USA: National Institute of Standards and Technology, 2011, doi: 10.18434/T4D303.

[28] COMSOL. *Multiphysics V. 6.1*. COMSOL AB, Stockholm, Sweden. Accessed: Oct. 10, 2023. [Online]. Available: https://www.comsol.com

[29] B. E. Schubert and D. Floreano, "Variable stiffness material based on rigid low-melting-point-alloy microstructures embedded in soft poly (dimethylsiloxane)(PDMS)," *RSC Adv.*, vol. 3, no. 46, pp. 24671–24679, 2013.

[30] C.-S. Park, K.-I. Joo, S.-W. Kang, and H.-R. Kim, "A PDMS-coated optical fiber Bragg grating sensor for enhancing temperature sensitivity," *J. Opt. Soc. Korea*, vol. 15, no. 4, pp. 329–334, Dec. 2011. [Online]. Available: https://opg.optica.org/josk/abstract.cfm?URI=josk-15-4-329

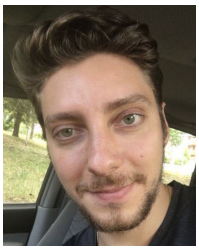

DAVIDE PRIVITERA received the bachelor's and master's degrees (cum laude) in computer and automation engineering from the University of Siena, Italy. Since 2016, he has been an Automation Engineer with Pharma Integration, where he contributes to the development of innovative robotics solutions in next-generation filling systems for pharmaceutical. In 2018, he assumed the role of the Head of Automation with Pharma Integration. In 2021, he embarked on a doctoral program with the University of Siena, focusing on the development of intelligent systems for Industry 4.0. His research interest includes studying methods to improve the accuracy of dosing systems used in the pharmaceutical industry.

STEFANO BELLISSIMA received the master's (cum laude) and Ph.D. degrees in physics from the University of Florence, Italy, in 2013 and 2016, respectively. From 2016 to 2019, he was a Research Fellow with the National Research Council, Sesto Fiorentino, Italy. He worked for the development of an innovative neutron spectrometer for the European Spallation Source, Lund, Sweden. Since 2019, he has been with the Automation Department, Pharma Integration, Siena, Italy, where he contributes to the development of new-generation robotic filling lines for the pharmaceutical sector. He is currently working on a project aimed at applying data science techniques to improve the performance of dosing systems. His research interests include condensed-matter physics with a focus on neutron scattering techniques and molecular dynamics simulation.

SANDRO BARTOLINI is currently an Associate Professor with the Department of Information Engineering and Mathematical Sciences, University of Siena, Italy. He has led and participated in various research and development projects. His main research interests include comprise: high-performance chip multiprocessors (CMPs), new approaches to productive programming of heterogeneous architectures (CPUs and GPUs), integrated photonics for CMPs, feedback-driven compiler optimizations for cache hierarchy performance and low power, and hardware accelerators. He is an Active Member of HiPEAC NoE. He is an Associate Editor of *EURASIP Journal of Embedded Systems*. He has been the Co-Guest Editor of *Transactions on High Performance Architectures and Compilation* (Springer) journal, and the *ACM Sigarch Computer Architecture Newsletter*.

Open Access funding provided by 'Università degli Studi di Siena' within the CRUI CARE Agreement